

Fig. 1. Immunohistochemical staining of pSTAT3 in HCC. **a** pSTAT3 was expressed in the nucleus. In nontumorous tissue, endothelial cells, bile duct epithelial cells and inflammatory cells were stained by pSTAT3 (left panel). $\times 100$. HCC cells were also stained (82.2%, right panel). $\times 100$. **b** Tumor cells of PVI and IM stained by pSTAT3. $\times 200$. **c** Comparison of pSTAT3 staining in primary

HCC, tumor cells of PVI and IM. pSTAT3 staining was significantly prominent in tumor cells of PVI and IM compared with primary HCC ($p < 0.05$). **d, e** pSTAT3 expression correlated with poor prognosis. OS (**d**) and DFS (**e**) curves for pSTAT3-positive and pSTAT3-negative groups in patients with HCC (**d**, $p = 0.0234$; **e**, $p = 0.0003$; log-rank test).

washed and incubated with horseradish peroxidase-conjugated secondary antibody (Cell Signaling Technology). Bands were visualized by the enhanced chemiluminescence system (GE Healthcare, UK).

Cell Growth Assay

PLC/PRF/5 and Huh7 cells were seeded at a density of 5×10^4 cells/24-well plates and maintained in conditioned medium for 24 h before stimulation. Viable cells were counted by trypan blue stain 48 h after stimulation with IL-6 (25 ng/ml).

Wound-Healing Assay

PLC/PRF/5 and Huh7 cells were seeded at a density of 5×10^4 cells/6-well plates. Approximately 24 h later, when the cells were 100% confluent, a sterile 100- μ l pipette tip was used to longitudi-

nally scratch a constant-diameter strip in the confluent monolayer. The medium and cell debris were aspirated away and replaced by 2 ml of fresh DMEM containing 1% FBS with or without IL-6 (25 ng/ml). Photographs were taken at 0 and 48 h after wounding by phase-contrast microscopy. For statistical analysis, three randomly selected points along each wound were marked, and the horizontal distance between the migrating cells and the initial wound was measured 48 h later.

Inhibition of STAT3

In both cell growth and wound-healing assays, PLC/PRF/5 and Huh7 cells were cultured in DMEM containing 1% FBS and IL-6 (25 ng/ml) with or without 100 nM S3I-201 (NSC 74859; Santa Cruz Biotechnology). S3I-201 was treated 30 min before IL-6 stimulation. DMSO was used for control.

Table 1. Comparison of pSTAT3 expression and clinicopathological findings

pSTAT3 expression	pSTAT3 negative (n = 65)	pSTAT3 positive (n = 36)	p value
<i>Clinical features</i>			
Sex, male/female	55/10	26/10	0.0849
Age, years	63.9±7.3	63.6±9.5	0.8726
HBsAg, +/-	14/51	8/28	0.9922
HCV Ab, +/-	42/23	23/13	0.9798
Cirrhosis	22/43	14/22	0.4990
AFP, ng/ml	852.4±308 [†]	20,673.4±11,688 [†]	0.0276*
DCP, mAU/ml	2,798.2±1,179.1 [†]	6,278.4±3,184.7 [†]	0.2217
<i>Pathological features</i>			
Tumor size, cm	3.7±2.2	5.1±3.2	0.0092*
Differentiation, poor/well and moderate	19/46	16/20	0.1253
Capsule formation	41/24	26/10	0.4619
Infiltration to the capsule	33/32	23/13	0.1681
Portal venous invasion, +/-	30/35	24/12	0.0687
Hepatic venous invasion, +/-	15/50	12/24	0.3031
Intrahepatic metastasis, +/-	18/47	18/18	0.0214*
MIB-1 LI, %	3.5±0.5	10.2±2.2	0.0002*
Bcl-XL, %	13.0±1.5	25.2±2.0	0.0001*

HBsAg = Hepatitis B surface antigen; HCV Ab = hepatitis C virus antibody; DCP = des-γ-carboxy prothorombin. * p < 0.05.

Statistical Analysis

Statistical analysis was carried out using Microsoft Excel software and JMP software (SAS Institute, Cary, N.C., USA). Comparison between pSTAT3 staining and clinicopathological findings or staining of other antibodies was evaluated by Pearson's χ^2 , Fisher's exact tests and the Mann-Whitney U test. Patient survival analysis including overall survival (OS) and disease-free survival (DFS) was calculated by the Kaplan-Meier method; differences were evaluated by the log-rank test. For multivariate analysis, the Cox proportional hazard model was used. Two-sided Student's t test was applied for analysis of in vitro data. Statistical analyses were considered significant at a p value < 0.05.

Results

pSTAT3 Expression in Clinical Samples

pSTAT3 was stained in the nuclei of HCC cells, normal endothelial cells, some bile duct epithelial cells and inflammatory cells. pSTAT3 nuclear staining in HCC

cells is displayed in figure 1a. The mean percentage of nuclear pSTAT3-positive cells in HCCs was 10.7% (range 0–82.0). The number of pSTAT3-positive and pSTAT3-negative samples was 36 and 65, respectively. We also examined pSTAT3 staining at the lesions of 19 portal venous invasions (PVI) and 12 intrahepatic metastases (IMs) in 101 cases. Fifteen of 19 PVI (78.9%) and 9 of 12 (75.0%) IMs were defined as pSTAT3-positive cases (fig. 1b). Positive rates in both lesions were significantly higher than those in the primary lesions (35.6%; p < 0.05; fig. 1c).

Comparison of pSTAT3 Expression and Clinicopathological Findings

A comparison of clinicopathological findings in pSTAT3-positive and pSTAT3-negative groups is summarized in table 1. The pSTAT3-positive group showed higher AFP (p = 0.0276), larger tumor size (p = 0.0092), more frequent IMs (p = 0.0214), a higher Ki-67 labeling index (LI; p = 0.0002), and more Bcl-XL-positive cells (p = 0.0001) than the pSTAT3-negative group, whereas no significant differences were noted with respect to sex, age, infection of hepatitis viruses, liver cirrhosis, PIVKA II (proteins induced by vitamin K absence or antagonist II), histological differentiation, capsule formation, infiltration to the capsule, and vessel invasion.

Survival Analysis after Surgery

The median follow-up period was 1,391 days (range 36–3,289). pSTAT3 expression was significantly correlated with OS and DFS (p = 0.0234 and 0.0003, respectively; fig. 1d, e). Univariate analyses indicated that high AFP (>100 ng/ml), large tumor size (>5 cm), PVI and IMs were prognostic factors for OS and male sex, hepatitis C virus infection, high AFP (>100 ng/ml) and IMs for DFS (table 2). Multivariate proportional hazard models revealed that high AFP and IMs were independent prognostic factors for OS and pSTAT3 expression and high AFP for DFS (table 2).

Tumor-Associated Macrophage Localization and pSTAT3 Expression of HCCs

CD163-positive cells were localized around the pSTAT3-positive HCC cells (fig. 2a). Figure 2b shows the boxplots of CD163-positive cells (mean ± SD: pSTAT3-negative group, 28.5 ± 15.4; pSTAT3-positive group, 42.6 ± 26.6). The pSTAT3-positive group (n = 36) showed statistically higher CD163-positive cells (p = 0.0013; fig. 2b) than the pSTAT3-negative group (n = 65). Furthermore, we analyzed the localization of CD163-posi-

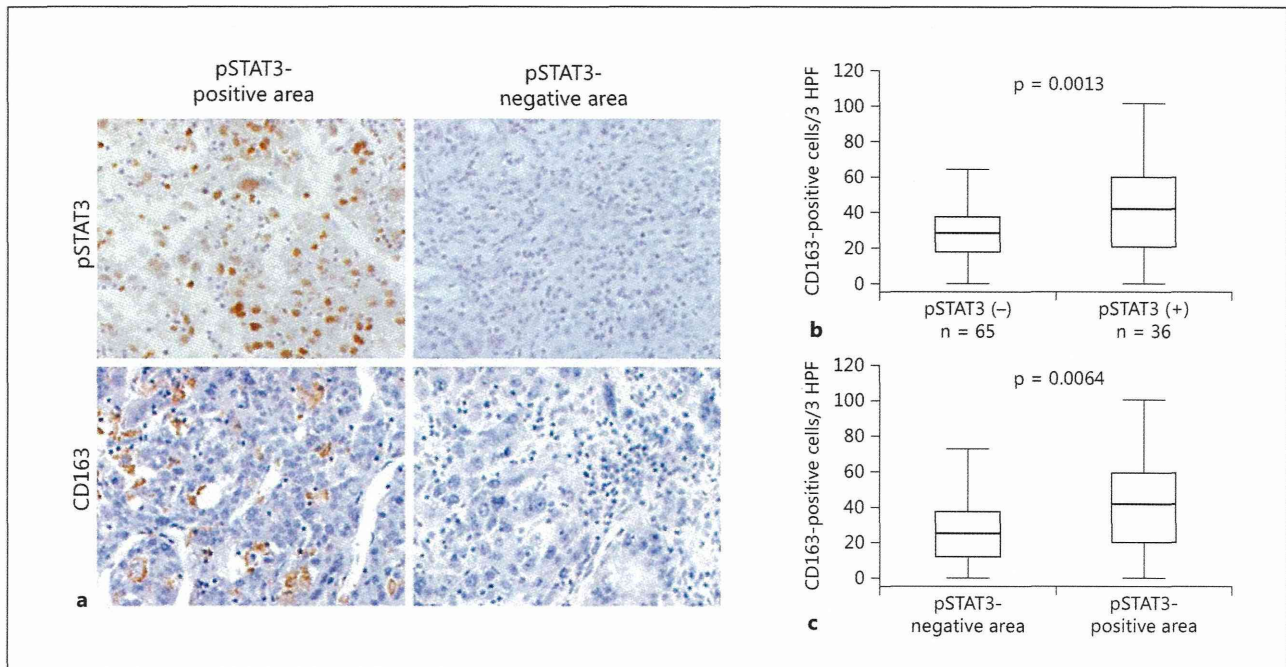


Fig. 2. Tumor-associated macrophages correlated with pSTAT3 expression in HCC. **a** Immunohistochemical staining of pSTAT3 and CD163 in the pSTAT3-positive and pSTAT3-negative area. $\times 200$. **b** Counts of CD163-positive cells between pSTAT3-positive

and pSTAT3-negative groups. **c** Counts of CD163-positive cells in areas of pSTAT3-positive and pSTAT3-negative HCC cells existed in the pSTAT3-positive group. HPF = High-power field.

Table 2. Survival analysis after surgery

Variable	Univariate analysis of OS		Multivariate analysis of OS		
	p value	hazard ratio	95% CI	p value	
pSTAT3 positive	0.0234*	1.104	0.465–2.683	0.8236	
AFP >100 ng/ml	0.0005*	2.968	1.294–7.026	0.0103*	
Tumor size >5 cm	0.0246*	1.489	0.610–3.578	0.3755	
Portal venous invasion	0.0422*	1.568	0.629–4.1265	0.3367	
Intrahepatic metastasis	0.0022*	2.668	1.186–6.194	0.0177*	

Variable	Univariate analysis of DFS		Multivariate analysis of DFS		
	p value	hazard ratio	95% CI	p value	
pSTAT3 positive	0.0003*	1.851	1.066–3.201	0.0288*	
Sex, male	0.0267*	0.978	0.515–1.790	0.9431	
HCV Ab (+)	0.0158*	1.672	0.948–3.096	0.0767	
AFP >100 ng/ml	0.0002*	2.070	1.218–3.476	0.0076*	
Intrahepatic metastasis	0.0012*	1.702	0.964–3.012	0.0664	

CI = Confidence interval; HCV Ab = hepatitis C virus antibody. * $p < 0.05$.

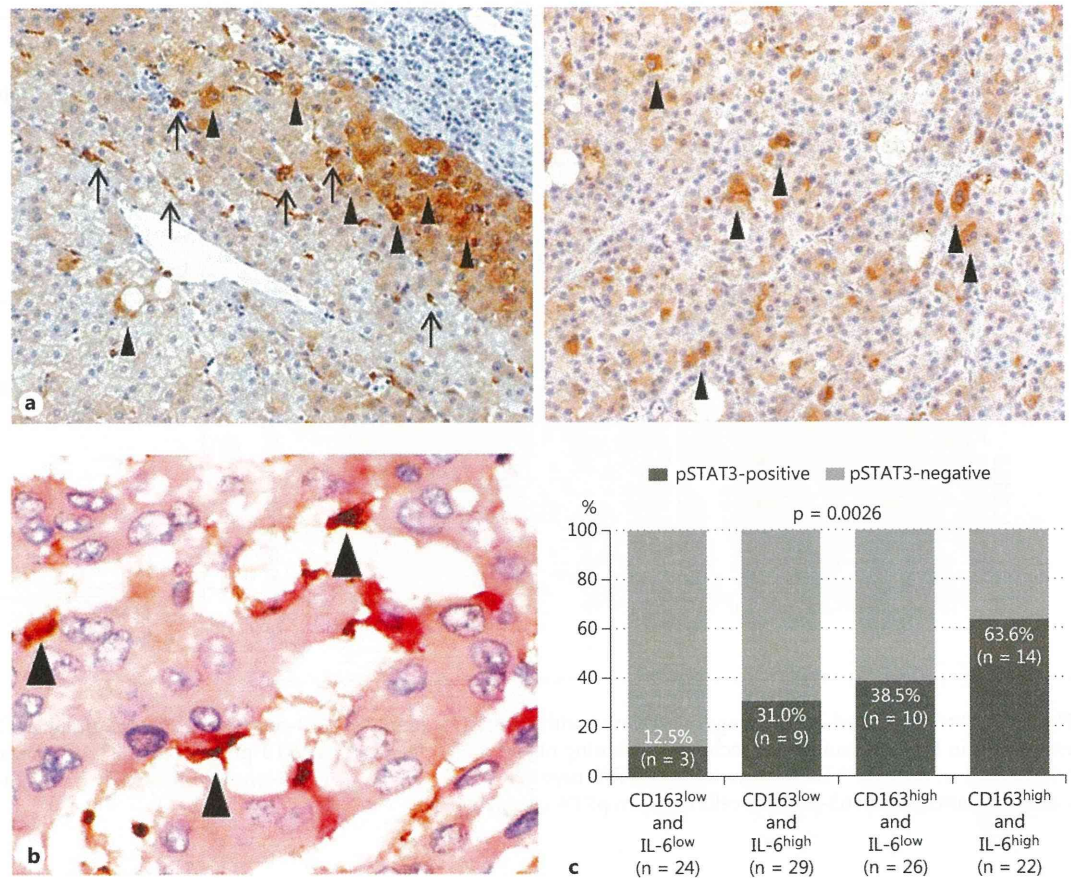


Fig. 3. Tumor-associated macrophages expressed IL-6. **a** Immunohistochemical staining of IL-6 in HCC. $\times 200$. Not only macrophages (arrows, left panel) but also some hepatocytes (arrowheads, left panel) and some tumor cells (arrowheads, right panel) showed immunoreactivities for IL-6. **b** Double staining of IL-6 (red) and CD163 (brown). $\times 400$. Double-positive cells (arrowheads) were frequently seen in the tumor. **c** Correlation between pSTAT3-positive and IL-6/CD163-positive staining.

tive cells in areas where pSTAT3-positive and pSTAT3-negative HCC cells existed in the pSTAT3-positive group ($n = 36$), and figure 2c shows the boxplots of the analyses (mean \pm SD: pSTAT3-negative area, 27.7 ± 17.9 ; pSTAT3-positive area, 42.6 ± 26.6). In the pSTAT3-positive group, CD163-positive cells in areas where pSTAT3-positive HCC cells existed were statistically higher than in those where pSTAT3-negative HCC cells existed ($p = 0.0064$; fig. 2c).

Cytokine Expression of Macrophages

IL-6 was stained in some macrophages, HCC cells and normal hepatocytes (fig. 3a). According to the double staining of CD163 and IL-6, CD163-positive cells (tumor-associated macrophages) expressed IL-6 (fig. 3b).

We divided them into two by the median values of positive macrophages of IL-6 and CD163, and thereby classified the 101 cases into four groups such as CD163^{low} and IL-6^{low}, CD163^{low} and IL-6^{high}, CD163^{high} and IL-6^{low}, and CD163^{high} and IL-6^{high}. HCCs containing high infiltration of IL-6- and CD163-positive macrophages exhibited a significantly higher rate of positive staining for pSTAT3 (fig. 3c).

IL-6 Stimulates Cell Proliferation and Migration of Human HCC Cell Lines

IL-6 stimulation increased the levels of pSTAT3 in both PLC/PRF/5 and Huh7 HCC cell lines (fig. 4a). IL-6 stimulation resulted in higher proliferation (fig. 4b) and greater migration distance (fig. 4c) versus control. S3I-

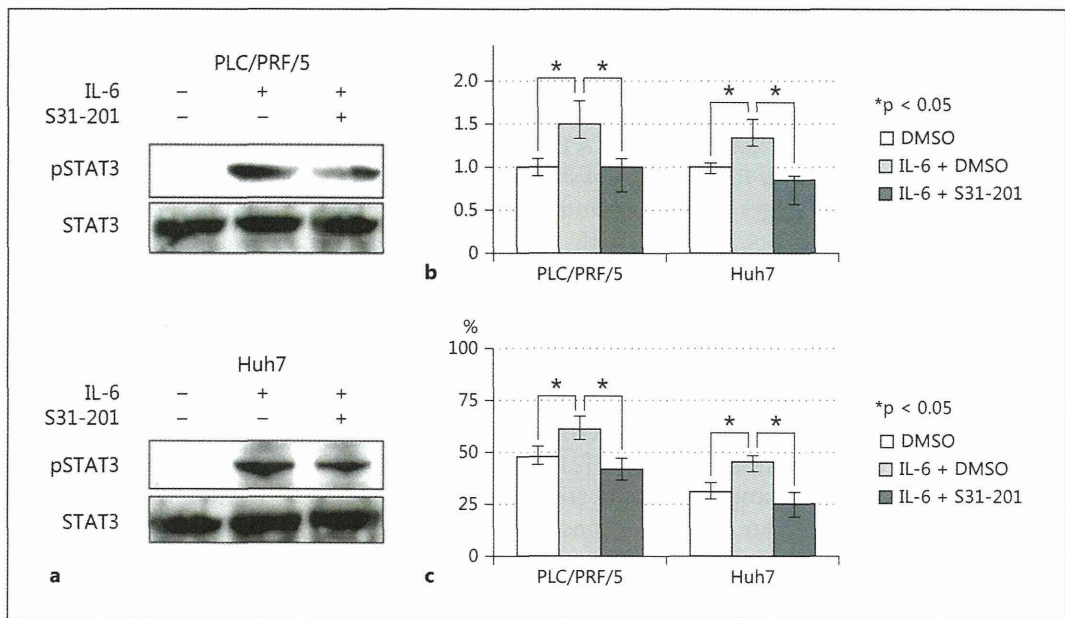


Fig. 4. IL-6 stimulation activated STAT3 signaling and promoted cell proliferation and migration in HCC cell lines. **a** PLC/PRF/5 (upper panel) and Huh7 (lower panel) were treated with 25 ng/ml IL-6 for 30 min. **b** PLC/PRF/5 and Huh7 were cultured with 25 ng/ml IL-6, 100 nM S31-201 and conditioned medium (1% FBS); cell proliferation was evaluated 48 h after IL-6 stimulation. Control set at 1. **c** PLC/PRF/5 and Huh7 were cultured with 25 ng/ml IL-6, 100 nM S31-201 and conditioned medium (1% FBS), and wound-healing assay was evaluated 48 h thereafter.

201, a STAT3 inhibitor, inhibited IL-6-induced STAT3 phosphorylation (fig. 4a) and decreased proliferation and migration of HCC cell lines (fig. 4b, c).

Discussion

Our results suggest that macrophage infiltration into HCC tissue stimulates tumor cells via STAT3 signaling. In the present study, pSTAT3-positive HCCs show malignant behavior and confer poor prognosis because of their high abilities of cell proliferation and migration. We found that high pSTAT3 expression was significantly correlated with larger tumor size, higher Ki-67 LI, higher Bcl-XL expression and greater frequency of IMs, and higher pSTAT3 expression was observed in the lesions of IMs and PVIs than in the primary lesions. STAT3 activation upregulates cell cycle-related, antiapoptotic and invasion genes [8–13, 26, 27]. In our results, large tumor size and high Ki-67 LI indicated cell cycle progression, high Bcl-XL expression indicated antiapoptotic function, and frequent IMs indicated invasive capacity. Furthermore, high pSTAT3 expression in the lesions of IMs and

PVIs suggests that the tumor cells with STAT3 activation in the primary lesions tended to invade the vessels and metastasize to the other liver sites. Xie et al. [26, 27] reported that activated STAT3 regulated tumor invasion of melanoma cells by regulating the gene transcription of matrix metalloproteinase 2. These results suggest that pSTAT3 expression plays an important role for cell survival and migration in HCC, consistent with previous studies in HCC [14, 17, 28, 29] and other tumors [5, 8–12, 26, 27, 30].

In recent years, it has been recognized that the balance between tumor immunity and tumor progression is important [31]. The present study revealed that tumor-associated macrophages are important for pSTAT3 expression of tumor cells. First, CD163-positive cells around pSTAT3-positive HCC cells were statistically more prevalent than around pSTAT3-negative HCC cells. Some of the CD163-positive cells expressed IL-6 in HCC tissue, and STAT3 was phosphorylated by IL-6 stimulation in vitro. These results suggest that tumor-associated macrophages can activate HCC cells via STAT3 signaling by IL-6 expression. However, CD-163-positive cells were detected not only in the pSTAT3-negative tumor area but

also in the pSTAT3-positive tumor area and in noncancerous liver tissue. IL-6-secreting tumor-associated macrophages may be part of the CD163-positive cells, and the CD163-positive cells in the pSTAT3-positive tumor area were more stained by IL-6 than in the pSTAT3-negative tumor area and normal liver tissue (data not shown). Tumor-associated macrophages express immunosuppressive cytokines including IL-4, IL-6, IL-10, IL-17, and IL-23 [32, 33]. These cytokines activate immunosuppressive inflammatory cells such as other tumor-associated macrophages, helper T cells and regulatory T cells and suppress antitumor inflammatory cells such as lymphocytes, natural killer cells and dendritic cells [34–36]. Kuang et al. [32] showed that tumor-associated macrophages expressed IL-6 in vitro, whereas Ding et al. [21] reported that tumor-associated macrophage was correlated with poor prognosis in HCC. Our results are consistent with these previous reports.

Both proliferation and migration of PLC/RPF/5 and Huh7 were increased following IL-6 stimulation and STAT3 phosphorylation. On the other hand, IL-6 was expressed in not only macrophages but also in HCC cells. STAT3 can be activated through autocrine signaling in HCC cells; moreover, other cytokines and growth factors might activate STAT3 of tumor cells [22–24]. It is very difficult to exclude activation of STAT3 by the autocrine manner. In our data, STAT3 activation of HCC cells was not correlated with surrounding IL-6-positive normal hepatocytes and HCC cells but it was correlated with the infiltration of CD-163-positive cells (fig. 2). Thus, we thought that the IL-6 secretion of tumor-associated macrophages is more important for STAT3 activation of HCC cells than the IL-6 secretion of other cells.

Recently, STAT3 phosphorylation inhibitors such as S3I-201 have been investigated in vitro and in vivo [28–30]. Avella et al. [37] reported that STAT3 can be one of the targets of chemoimmunotherapies. In our study, S3I-201 inhibited IL-6-induced STAT3 phosphorylation in vitro and decreased cell proliferation and migration. The inhibition of tumor-associated macrophages as therapeutic strategy of malignancy has been investigated, too [38–41]. Therefore, it is very important to suppress tumor-associated macrophage activation and STAT3 signaling in the treatment of HCC. Furthermore, tumor-associated macrophage activation requires STAT3 signaling [22]. We consider that the STAT3 inhibitor may suppress STAT3 activation in both tumor cells and tumor-associated macrophages, release antitumor immune systems from suppression by tumor-associated macrophages and thereby control tumor progression of HCC. Therefore, STAT3 signaling is a feasible therapeutic target for HCC.

In conclusion, STAT3 activation is one of the prognostic factors in HCC. Tumor-associated macrophage expresses IL-6 and can activate STAT3 signaling of HCC cells, resulting in their cell proliferation, antiapoptosis and migration. In the future, HCC may be suppressed by inhibition of STAT3 signaling of tumor cells and tumor-associated macrophages.

Disclosure Statement

The authors have no conflicts of interest.

References

- Llovet JM, Burroughs A, Bruix J: Hepatocellular carcinoma. *Lancet* 2003;362:1907–1917.
- Shirabe K, Kanematsu T, Matumata T, Adachi E, Akazawa K, Sugimachi K: Factors linked to early recurrence of small hepatocellular carcinoma after hepatectomy: univariate and multivariate analyses. *Hepatology* 1991; 14:802–805.
- Taura K, Ikai I, Hatano E, Fujii H, Uyama N, Shimahara Y: Implication of frequent local ablation therapy for intrahepatic recurrence in prolonged survival of patients with hepatocellular carcinoma undergoing hepatic resection: an analysis of 610 patients over 16 years old. *Ann Surg* 2006;244:265–273.
- Llovet JM, Ricci S, Mazzaferro V, Hilgard P, Gane E, Blanc JF, de Oliveira AC, Santoro A, Raoul JL, Forner A, Schwartz M, Porta C, Zeuzem S, Bolondi L, Greten TF, Galle PR, Seitz JF, Borbath I, Häussinger D, Giannaris T, Shan M, Moscovici M, Voliotis D, Bruix J, SHARP Investigators Study Group: Sorafenib in advanced hepatocellular carcinoma. *N Engl J Med* 2008;359:378–390.
- Bromberg JF, Wrzeszczynska MH, Devgan G, Zhao Y, Pestell RG, Albanese C, Darnell JE Jr: Stat3 as an oncogene. *Cell* 1999;98:295–303.
- Al Zaid Siddiquee K, Turkson J: STAT3 as a target for inducing apoptosis in solid and hematological tumors. *Cell Res* 2008;18:254–267.
- Murray PJ: The JAK-STAT signaling pathway: input and output integration. *J Immunol* 2007;178:2623–2629.
- Berishaj M, Gao SP, Ahmed S, Leslie K, Al-Ahmadie H, Gerald WL, Bornmann W, Bromberg JF: Stat3 is tyrosine-phosphorylated through the interleukin-6/glycoprotein 130/Janus kinase pathway in breast cancer. *Breast Cancer Res* 2007;9:R32.

- 9 Lin Q, Lai R, Chirieac LR, Li C, Thomazy VA, Grammatikakis I, Rassidakis GZ, Zhang W, Fujio Y, Kunisada K, Hamilton SR, Amin HM: Constitutive activation of JAK3/STAT3 in colon carcinoma tumors and cell lines: inhibition of JAK3/STAT3 signaling induces apoptosis and cell cycle arrest of colon carcinoma cells. *Am J Pathol* 2005;167:969–980.
- 10 Song L, Turkson J, Karras JG, Jove R, Haura EB: Activation of Stat3 by receptor tyrosine kinases and cytokines regulates survival in human non-small cell carcinoma cells. *Oncogene* 2003;22:4150–4165.
- 11 Greten FR, Weber CK, Greten TF, Schneider G, Wagner M, Adler G, Schmid RM: Stat3 and NF-kappaB activation prevents apoptosis in pancreatic carcinogenesis. *Gastroenterology* 2002;123:2052–2063.
- 12 Ni Z, Lou W, Leman ES, Gao AC: Inhibition of constitutively activated Stat3 signaling pathway suppresses growth of prostate cancer cells. *Cancer Res* 2000;60:1225–1228.
- 13 Kreis S, Munz GA, Haan S, Heinrich PC, Behrmann I: Cell density dependent increase of constitutive signal transducers and activators of transcription 3 activity in melanoma cells is mediated by Janus kinases. *Mol Cancer Res* 2007;5:1331–1341.
- 14 Rajendran P, Ong TH, Chen L, Li F, Shanmugam MK, Vali S, Abbasi T, Kapoor S, Sharma A, Kumar AP, Hui KM, Sethi G: Suppression of signal transducer and activator of transcription 3 activation by butein inhibits growth of human hepatocellular carcinoma in vivo. *Clin Cancer Res* 2011;17:1425–1439.
- 15 Yang SF, Wang SN, Wu CF, Yeh YT, Chai CY, Chunag SC, Sheen MC, Lee KT: Altered p-STAT3 (Tyr705) expression is associated with histological grading and intratumour microvessel density in hepatocellular carcinoma. *J Clin Pathol* 2007;60:642–648.
- 16 Ogata H, Kobayashi T, Chinen T, Takaki H, Sanada T, Minoda Y, Koga K, Takaesu G, Maehara Y, Iida M, Yoshimura A: Deletion of the SOCS3 gene in liver parenchymal cells promotes hepatitis-induced hepatocarcinogenesis. *Gastroenterology* 2006;131:179–193.
- 17 Pollard JW: Tumour-educated macrophages promote tumour progression and metastasis. *Nat Rev Cancer* 2004;4:71–78.
- 18 Lewis CE, Pollard JW: Distinct role of macrophages in different tumor microenvironments. *Cancer Res* 2006;66:605–612.
- 19 Hasita H, Komohara Y, Okabe H, Masuda T, Ohnishi K, Lei XF, Beppu T, Baba H, Takeya M: Significance of alternatively activated macrophages in patients with intrahepatic cholangiocarcinoma. *Cancer Sci* 2010;101:1913–1919.
- 20 Siveen KS, Kuttan G: Role of macrophages in tumor progression. *Immunol Letter* 2009;123:97–102.
- 21 Ding T, Xu J, Wang F, Shi M, Zhang Y, Li SP, Zheng L: High tumor-infiltrating macrophage density predicts poor prognosis in patients with primary hepatocellular carcinoma after resection. *Hum Pathol* 2009;40:381–389.
- 22 Fujiwara Y, Komohara Y, Ikeda T, Takeya M: Corosolic acid inhibits glioblastoma cell proliferation by suppressing the activation of signal transducer and activator of transcription-3 and nuclear factor-kappa B in tumor cells and tumor-associated macrophages. *Cancer Sci* 2011;102:206–211.
- 23 Takaishi K, Komohara Y, Tashiro H, Ohtake H, Nakagawa T, Katabuchi H, Takeya M: Involvement of M2-polarized macrophages in the ascites from advanced epithelial ovarian carcinoma in tumor progression via Stat3 activation. *Cancer Sci* 2010;101:2128–2136.
- 24 Domínguez-Soto A, Sierra-Filardi E, Puig-Kröger A, Pérez-Maceda B, Gómez-Aguado F, Corcuera MT, Sánchez-Mateos P, Corbí AL: Dendritic cell-specific ICAM-3-grabbing nonintegrin expression on M2-polarized and tumor-associated macrophages is macrophage-CSF dependent and enhanced by tumor-derived IL-6 and IL-10. *J Immunol* 2011;186:2192–2200.
- 25 Komohara Y, Ohnishi K, Kuratsu J, Takeya M: Possible involvement of the M2 anti-inflammatory macrophage phenotype in growth of human gliomas. *J Pathol* 2008;216:15–24.
- 26 Xie TX, Wei D, Liu M, Gao AC, Ali-Osman F, Sawaya R, Huang S: Stat3 activation regulates the expression of matrix metalloproteinase-2 and tumor invasion and metastasis. *Oncogene* 2004;23:3550–3560.
- 27 Xie TX, Huang FJ, Aldape KD, Kang SH, Liu M, Gershenwald JE, Xie K, Sawaya R, Huang S: Activation of Stat3 in human melanoma promotes brain metastasis. *Cancer Res* 2006;66:3188–3196.
- 28 Lin L, Amin R, Gallicano GI, Glasgow E, Joganoori W, Jessup JM, Zasloff M, Marshall JL, Shetty K, Johnson L, Mishra L, He AR: The STAT3 inhibitor NSC 74859 is effective in hepatocellular cancers with disrupted TGF-beta signaling. *Oncogene* 2009;28:961–972.
- 29 Choudhari SR, Khan MA, Harris G, Picker D, Jacob GS, Block T, Shailubhai K: Deactivation of Akt and STAT3 signalling promotes apoptosis, inhibits proliferation, and enhances the sensitivity of hepatocellular carcinoma cells to an anticancer agent, Atiprimod. *Mol Cancer Ther* 2007;6:112–121.
- 30 Lin L, Hutzen B, Zuo M, Ball S, Deangelis S, Foust E, Pandit B, Innat MA, Shenoy SS, Kulp S, Li PK, Li C, Fuchs J, Lin J: Novel STAT3 phosphorylation inhibitors exhibit potent growth-suppressive activity in pancreatic and breast cancer cells. *Cancer Res* 2010;70:2445–2454.
- 31 Korangy F, Höchst B, Manns MP, Greten TF: Immune responses in hepatocellular carcinoma. *Dig Dis* 2010;28:150–154.
- 32 Kuang DM, Peng C, Zhao Q, Wu Y, Chen MS, Zheng L: Activated monocytes in peritumoral stroma of hepatocellular carcinoma promote expansion of memory T helper 17 cells. *Hepatology* 2010;51:154–164.
- 33 Kortylewski M, Xin H, Kujawski M, Lee H, Liu Y, Harris T, Drake C, Pardoll D, Yu H: Regulation of the IL-23 and IL-23 balance by Stat3 signaling in the tumor microenvironment. *Cancer Cell* 2009;15:114–123.
- 34 Kuang DM, Zhao Q, Peng C, Xu J, Zhang JP, Wu C, Zheng L: Activated monocytes in peritumoral stroma of hepatocellular carcinoma foster immune privilege and disease progression through PD-L1. *J Exp Med* 2009;206:1327–1337.
- 35 Wu K, Kryczek I, Chen L, Zou W, Welling TH: Kupffer cell suppression of CD8+ T cells in human hepatocellular carcinoma is mediated by B7-H1/programmed death-1 interactions. *Cancer Res* 2009;69:8067–8075.
- 36 Niemand C, Nimmesger A, Haan S, Fischer P, Schaper F, Rössaint R, Heinrich PC, Müller-Newen G: Activation of STAT3 by IL-6 and IL-10 in primary human macrophages is differentially modulated by suppressor of cytokine signaling 3. *J Immunol* 2003;170:3263–3272.
- 37 Avella DM, Li G, Schell TD, Liu D, Zhang SS, Lou X, Berg A, Kimchi ET, Tagaram HR, Yang Q, Shereef S, Garcia LS, Kester M, Isom HC, Rountree CB, Staveley-O'Carroll KF: Regression of established hepatocellular carcinoma is induced by chemioimmunotherapy in an orthotopic murine model. *Hepatology* 2012;55:141–152.
- 38 Zhang W, Zhu XD, Sun HC, Xiong YQ, Zhuang PY, Xu HX, Kong LQ, Wang L, Wu WZ, Tang ZY: Depletion of tumor-associated macrophages enhances the effect of sorafenib in metastatic liver cancer models by antimetastatic and antiangiogenic effects. *Clin Cancer Res* 2010;16:3420–3430.
- 39 Luo Y, Zhou H, Krueger J, Kaplan C, Lee SH, Dolman C, Markowitz D, Wu W, Liu C, Reisfeld RA, Xiang R: Targeting tumor-associated macrophages as a novel strategy against breast cancer. *J Clin Invest* 2006;116:2132–2141.
- 40 Huang Y, Snuderl M, Jain RK: Polarization of tumor-associated macrophages: a novel strategy for vascular normalization and antitumor immunity. *Cancer Cell* 2011;19:1–2.
- 41 Wu WY, Li J, Wu ZS, Zhang CL, Meng XL: STAT3 activation in monocytes accelerates liver cancer progression. *BMC Cancer* 2011;11:506.

Identification of Novel Serum Biomarkers of Hepatocellular Carcinoma Using Glycomic Analysis

Toshiya Kamiyama,¹ Hideki Yokoo,¹ Jun-Ichi Furukawa,² Masaki Kurogochi,² Tomoaki Togashi,² Nobuaki Miura,² Kazuaki Nakanishi,¹ Hirofumi Kamachi,³ Tatsuhiko Kakisaka,¹ Yosuke Tsuruga,¹ Masato Fujiyoshi,¹ Akinobu Taketomi,¹ Shin-Ichiro Nishimura,² and Satoru Todo³

The altered *N*-glycosylation of glycoproteins has been suggested to play an important role in the behavior of malignant cells. Using glycomics technology, we attempted to determine the specific and detailed *N*-glycan profile for hepatocellular carcinoma (HCC) and investigate the prognostic capabilities. From 1999 to 2011, 369 patients underwent primary curative hepatectomy in our facility and were followed up for a median of 60.7 months. As normal controls, 26 living Japanese related liver transplantation donors were selected not infected by hepatitis B and C virus. Their mean age was 40.0 and 15 (57.7%) were male. We used a glycoblotting method to purify *N*-glycans from preoperative blood samples from this cohort (10 μ L serum) which were then identified and quantified using mass spectrometry (MS). Correlations between the *N*-glycan levels and the clinicopathologic characteristics and outcomes for these patients were evaluated. Our analysis of the relative areas of all the sugar peaks identified by MS, totaling 67 *N*-glycans, revealed that a proportion had higher relative areas in the HCC cases compared with the normal controls. Fourteen of these molecules had an area under the curve of greater than 0.80. Analysis of the correlation between these 14 *N*-glycans and surgical outcomes by univariate and multivariate analysis identified G2890 (*m/z* value, 2890.052) as a significant recurrence factor and G3560 (*m/z* value, 3560.295) as a significant prognostic factor. G2890 and G3560 were found to be strongly correlated with tumor number, size, and vascular invasion. **Conclusion:** Quantitative glycoblotting based on whole serum *N*-glycan profiling is an effective approach to screening for new biomarkers. The G2890 and G3560 *N*-glycans determined by tumor glycomics appear to be promising biomarkers for malignant behavior in HCCs. (HEPATOLOGY 2013;00:000–000)

Hepatocellular carcinoma (HCC) is a common and fatal malignancy with a worldwide occurrence.¹ Liver resection has shown the highest level of control among the local treatments for HCC and is associated with a good survival rate.^{2,3} However, the recurrence rates for HCC are still high even when a curative hepatectomy is performed.⁴ Many factors associated with the prognosis and recurrence of HCC have now been reported. Vascular invasion of the portal vein and/or hepatic vein and tumor differentiation are important factors affecting survival and recurrence

in HCC cases after a hepatectomy.^{5,6} However, microvascular invasion and differentiation can only be detected by pathological examination just after a hepatectomy, and cannot be diagnosed preoperatively, and thus cannot be identified preoperatively either. Hence, the serum biomarkers alpha-fetoprotein (AFP) and protein induced by vitamin K absence-II (PIVKA-II) are used as prognostic markers^{7,8} and also as surrogate markers for microvascular invasion and tumor differentiation.^{9,10} AFP is associated with grade differentiation,¹¹ whereas PIVKA-II is related to vascular

Abbreviations: AFP, alpha-fetoprotein; AFP-L3, lens culinaris agglutinin-reactive fraction of alpha-fetoprotein; AUC, area under the curve; DFS, disease-free survival; HCC, hepatocellular carcinoma; ICGR15, indocyanin green retention rate at 15 minutes; PIVKA-II, protein induced by vitamin K absence or antagonism factor II; PS, patient survival; RF, risk factor; ROC, receiver operating characteristics.

From the ¹Department of Gastroenterological Surgery I, Hokkaido University Graduate School of Medicine, Hokkaido, Japan; ²Graduate School of Life Science and Frontier Research Center for Post-Genome Science and Technology, Hokkaido University, Hokkaido, Japan; ³Department of Transplantation Surgery, Hokkaido University Graduate School of Medicine, Hokkaido, Japan

Received May 8, 2012; accepted December 19, 2012.

Supported by grants for "Development of Systems and Technology for Advanced Measurement and Analysis (SENTAN)" from the Japan Science and Technology Agency (JST).

invasion.^{12,13} However, these tumor markers have limited sensitivity and are less predictive than microvascular invasion,^{14,15} which is the most potent determinant of recurrence and survival in HCC patients undergoing a hepatectomy.⁵ Therefore, new biomarkers that are more strongly associated with prognosis and recurrence in HCC than AFP or PIVKA-II are highly desirable.

Glycosylation is one of the most common posttranslational protein modifications. Alterations in the *N*-glycosylation profiles of glycoproteins have been suggested to play important roles in the proliferation, differentiation, invasion, and metastasis of malignant cells. Glycan species can be analyzed and characterized using mass spectrometry (MS) and the profiling of these molecules when they are secreted or shed from cancer cells is also performed. Hence, some glycoproteins have been suggested as biomarkers of human carcinomas such as ovarian cancer, breast cancer, and HCC.¹⁶⁻¹⁹ Of note, changes to the *N*-linked glycan modification of glycoproteins occur during the tumorigenesis and progression of HCC lesions. However, the correlation between the *N*-glycan profile and tumor-associated characteristics such as the degree of malignancy and prognosis has not been previously evaluated in HCC. Recently, we developed a novel glycomics method that facilitates high-throughput and large-scale glycome analysis using an automated glycan purification system, SweetBlot. This approach enables us to profile serum *N*-glycans quantitatively. Using this quantitative *N*-glycomics procedure by way of glycoblotting technology, which is both highly accurate and can be conducted on a large scale, we have previously evaluated the potential of using *N*-glycans as markers of the prognosis and recurrence of HCC.²⁰

In our current study we evaluated preoperative blood samples from an HCC patient cohort from which we purified serum *N*-glycans using our glycoblotting method.^{21,22} We performed *N*-glycan profiling using MS to search for factors related to prognosis and recurrence by analysis of patient outcomes in 369 consecutive HCC cases that had undergone a primary curative hepatectomy at our medical facility. Through this screen we sought to correlate *N*-glycan levels on glycoproteins with the clinicopathologic characteristics and the outcomes of HCC.

Patients and Methods

Patients. Between April 1999 and March 2011, 369 consecutive adult patients underwent a hepatectomy procedure for HCC at our center and this sample population was examined in the current study. Patients with extrahepatic metastases had been excluded from this cohort because the outcomes of a hepatectomy in these cases are typically very poor. The mean age of the patients in the final study group was 62.7 ± 10.6 years (range, 33-90), 301/369 (81.6%) cases were male, 176 (47.7%) were hepatitis B virus surface antigen-positive, 119 (32.2%) were hepatitis C virus antibody-positive, and 120 (32.5%) were designated as F4 based on the New Inuyama Classification system.²³ The preoperative serum AFP and PIVKA-II levels were simultaneously measured in the patients using standard methods at least 2 weeks before the hepatectomy at the time of the imaging studies. Among the 369 patients in the cohort, 358 (97.0%) were categorized as Child-Pugh class A. According to the TNM stage revised by the Liver Study Group of Japan in 2010,²⁴ 26 (7.0%) patients were in stage I, 172 (46.6%) in stage II, 111 (30.1%) in stage III, and 60 (16.3%) in stage IVA. The patients were followed up for a median of 60.7 months (range, 9.8-155.1). As a normal control group, 26 living related liver transplantation donors were selected. They were evaluated for eligibility as donors by liver function tests, measurements of the tumor markers AFP and PIVKA-II, and also by x-ray photographs of chest and abdomen and dynamic computed tomography (CT). Their mean age was 40.0 with a range of 20-48. Of 26 controls, 15 (57.7%) were male and 11 (42.3%) were female. All controls were Japanese and not infected by hepatitis B and C virus. This study was approved by the Institutional Review Board of the Hokkaido University, School of Advanced Medicine. Informed consent was obtained from each patient in accordance with the Ethics Committees Guidelines for our institution.

Experimental Procedures: Serum *N*-Glycomics by Way of Glycoblotting. *N*-glycans from serum samples were purified by glycoblotting using BlotGlycoH. These are commercially available synthetic polymer beads with high-density hydrazide groups (Sumitomo Bakelite,

Address reprint requests to: Toshiya Kamiyama, M.D., Department of Gastroenterological Surgery I, Hokkaido University Graduate School of Medicine, North 15, West 7, Kita-ku, Sapporo 060-8638 Japan. E-mail: t-kamiya@med.hokudai.ac.jp; fax: +81-11-717-7515.

Copyright © 2013 by the American Association for the Study of Liver Diseases.

View this article online at wileyonlinelibrary.com.

DOI 10.1002/hep.26262

Potential conflict of interest: Nothing to report.

Tokyo, Japan). All procedures used the SweetBlot automated glycan purification system containing a 96-well plate platform (System Instruments, Hachioji, Japan).

Enzymatic Degradation of Serum N-Glycans.

Each 10- μ L serum sample aliquot was dissolved in 50 μ L of a 106-mM solution of ammonium bicarbonate containing 12 mM 1,4-dithiothreitol and 0.06% 1-propanesulfonic acid, 2-hydroxyl-3-myristamido (Wako Pure Chemical Industries, Osaka, Japan). After incubation at 60°C for 30 minutes, 123 mM iodoacetamide (10 μ L) was added to the mixtures followed by incubation in the dark at room temperature to enable reductive alkylation. After 60 minutes, the mixture was treated with 200 U of trypsin (Sigma-Aldrich, St. Louis, MO) at 37°C for 2 hours, followed by heat-inactivation of the enzyme at 90°C for 10 minutes. After cooling to room temperature, the N-glycans were released from the tryptic glycopeptides by incubation with 325 U of PNGase F (New England BioLabs, Ipswich, MA) at 37°C for 6 hours.

N-Glycan Purification and Modification by Glycoblotting. Glycoblotting of sample mixtures containing whole serum N-glycans was performed in accordance with previously described procedures. Commercially available BlotGlyco H beads (500 μ L) (10 mg/ml suspension; Sumitomo Bakelite) were aliquoted into the wells of a MultiScreen Solvinert hydrophilic PTFE (polytetrafluoroethylene) 96-well filter plate (EMD Millipore, Billerica, MA). After removal of the water using a vacuum pump, 20 μ L of PNGase F-digested samples were applied to the wells, followed by the addition of 180 μ L of 2% acetic acid in acetonitrile. The filter plate was then incubated at 80°C for 45 minutes to capture the N-glycans onto the beads by way of a chemically stable and reversible hydrazone bond. The beads were then washed using 200 μ L of 2 M guanidine-HCl in 10 mM ammonium bicarbonate, followed by washing with the same volume of water and of 1% triethyl amine in methanol. Each washing step was performed twice. The N-glycan linked beads were next incubated with 10% acetic anhydride in 1% triethyl amine in methanol for 30 minutes at room temperature so that unreacted hydrazide groups would become capped by acetylation. After capping, the reaction solution was removed under a vacuum and the beads were serially washed with 2×200 μ L of 10 mM HCl, 1% triethyl amine in methanol, and dioxane. This is a pretreatment for sialic acid modification. On-bead methyl esterification of carboxyl groups in the sialic acids was carried out with 100 μ L of 100 mM 3-methyl-1-*P*-tolyltriazene (Tokyo Chemical Industry, Tokyo, Japan) in dioxane at 60°C for 90

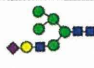
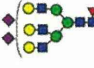
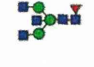
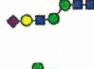
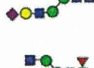
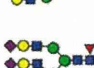

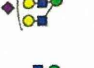
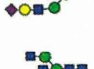
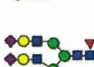



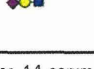
minutes to dryness. After methyl esterification of the more stable glycans, the beads were serially washed in 200 μ L of dioxane, water, 1% triethyl amine in methanol, and water. The captured glycans were then subjected to a *trans*-iminization reaction with BOA (O-benzylhydroxylamine) (Tokyo Chemical Industry) reagent for 45 minutes at 80°C. After this reaction, 150 μ L of water was added to each well, followed by the recovery of derivatized glycans under a vacuum.

Matrix-Assisted Laser Desorption Ionization, Time-of-Flight (MALDI-TOF) and TOF/TOF Analysis. The N-glycans purified by glycoblotting were directly diluted with α -cyano-4-hydroxycinnamic acid diethylamine salt (Sigma-Aldrich) as ionic liquid matrices and spotted onto the MALDI target plate. The analytes were then subjected to MALDI-TOF MS analysis using an Ultraflex time-of-flight mass spectrometer III (Bruker Daltonics, Billerica, MA) in reflector, positive ion mode and typically summing 1,000 shots. The N-glycan peaks in the MALDI-TOF MS spectra were selected using FlexAnalysis v. 3 (Bruker Daltonics). The intensity of the isotopic peak of each glycan was normalized using 40 μ M of internal standard (disialyloctasaccharide, Tokyo Chemical Industry) for each status, and its concentration was calculated from a calibration curve using human serum standards. The glycan structures were estimated using the GlycoMod Tool (<http://br.expasy.org/tools/glycomod/>), so that our system could quantitatively measure 67 N-glycans.

Hepatectomy. Anatomical resection is defined as a resection in which lesion(s) are completely removed on the basis of Couinaud's classification (segmentectomy, sectionectomy, and hemihepatectomy or more) in patients with a tolerable functional reserve. Nonanatomical partial, but complete resection was achieved in all of our cases. R0 resections were performed while the resection surface was found to be histologically free of HCC. The indocyanin green retention rate at 15 minutes was measured in each case to evaluate the liver function reserve, regardless of the presence or absence of cirrhosis.

HCC Recurrence. For the first 2 years after the hepatectomy procedure, the HCC patients in our cohort were monitored every 3 months using liver function tests, measurements of the tumor markers AFP and protein induced by PIVKA-II, and also by ultrasonography and dynamic CT. At 2 years postsurgery, routine CT was performed only once in 4 months. If recurrence was suspected, both CT and magnetic resonance imaging (MRI) were performed and, if necessary, CT during angiography and bone scintigraphy were undertaken.

Table 1. List of the 14 Serum N-Glycans That Were Evaluated to be Specific for Hepatocellular Carcinoma Compared with Normal Controls by Receiver Operating Characteristic (ROC) Analysis

N-glycans	m/z		Specificity (%)	Sensitivity (%)	Cutoff Value	AUC
G2032	2032.724		100	86.45	1.115	0.968
G2890	2890.052		92.31	82.66	0.844	0.91
G1793	1793.672		92.31	75.61	1.963	0.9
G1708	1708.619		88.46	77.51	0.604	0.896
G1870	1870.672		88.46	75.88	2.886	0.873
G1955	1955.724		100	59.89	3.913	0.873
G3195	3195.163		92.31	71.27	6.109	0.864
G3560	3560.295		88.46	71.27	0.091	0.851
G2114	2114.778		88.46	75.88	2.208	0.839
G1809	1809.666		84.62	72.9	0.679	0.838
G3341	3341.221		84.62	69.92	0.086	0.821
G1590	1590.592		80.77	69.92	10.696	0.817
G1362	1362.481		65.38	87.26	1.381	0.813
G3865	3865.407		92.31	56.37	0.121	0.812

The area-under-the-curve (AUC) values of these 14 serum N-glycan were greater than 0.80. These glycan structures are represented with the symbol nomenclature explained in <http://www.functionalglycomics.org/static/consortium/Nomenclature.shtml>.

This enabled a precise diagnosis of the site, number, size, and invasiveness of any recurrent lesions.

Statistics. The specificity, the sensitivity, cutoff, and AUC (area under the curve) values of selected N-glycans are shown in Table 1. This ROC (receiver operating characteristics) analysis was carried out using R v. 2.12.1. The patient survival (PS) and disease-free

survival rates (DFS) were determined using the Kaplan-Meier method and compared between groups by the log-rank test. Univariate analysis of variables was also performed, and selected variables using Akaike's Information Criterion (AIC)²⁵ were analyzed with the Cox proportional hazard model for multivariate analysis. Statistical analyses were performed using

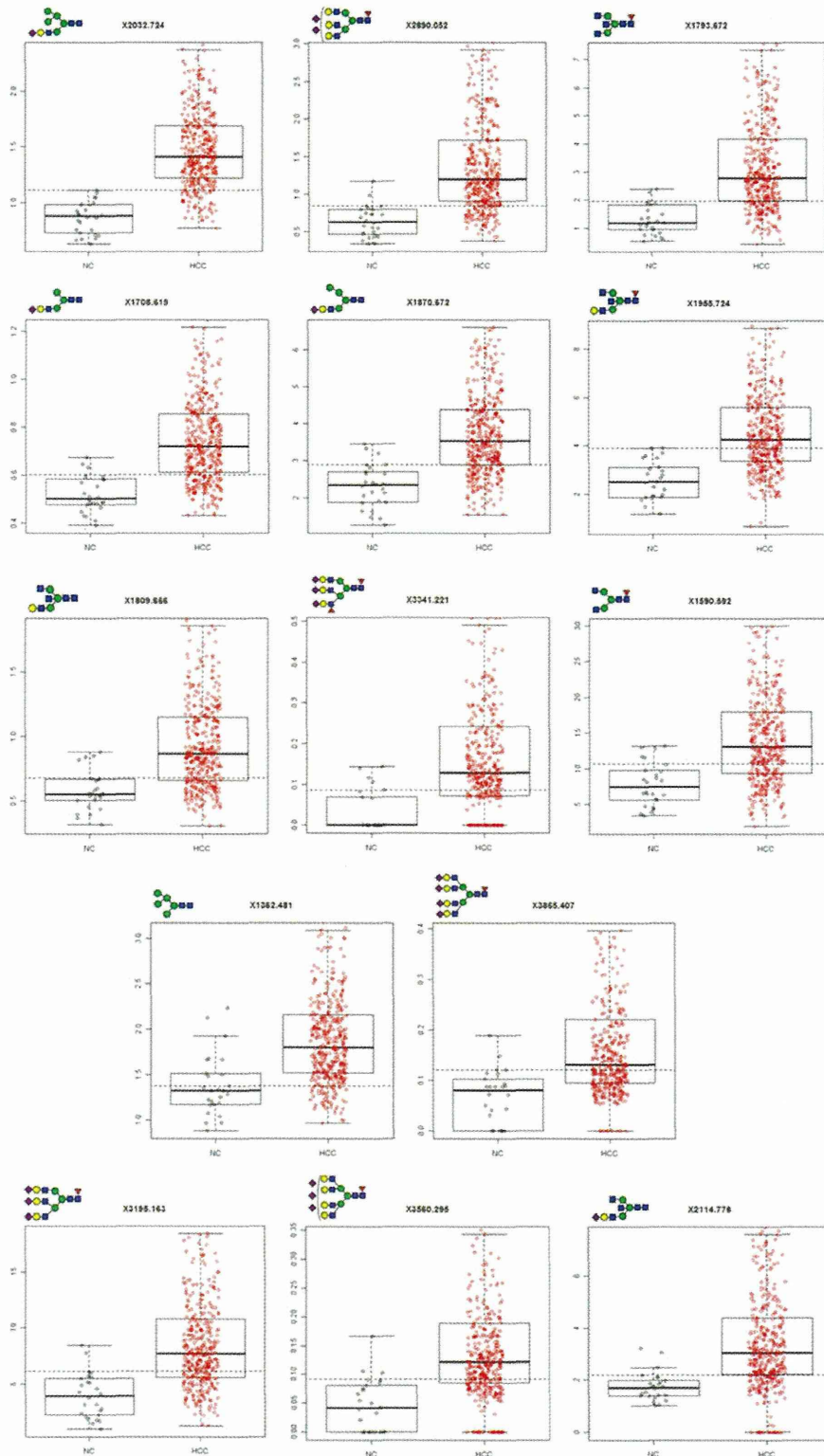


Fig. 1. Boxplots of the disease-free individuals (NC) and HCC patients for the selected 14 N-glycans. The dotted lines in the graphs represent the cutoff values determined in this analysis. These graphs were drawn using R v. 2.12.1.

Table 2. Univariate Analysis of Predictive Values (the Selected 14 N-Glycans) of Patient Survival (PS) and Disease-Free Survival (DFS)

		(n)	PS Hazard Ratio	PS P-value	DFS Hazard Ratio	DFS P-value
G2032	Low	206	1	0.9362	1	0.1054
	High	163	1.017		1.243	
G2890	Low	152	1	<0.0001	1	0.0001
	High	217	3.044		1.705	
G1793	Low	112	1	0.6829	1	0.2897
	High	257	1.095		1.168	
G1708	Low	145	1	0.0016	1	0.0043
	High	224	2.017		1.485	
G1870	Low	151	1	0.5552	1	0.4008
	High	218	1.132		1.122	
G1955	Low	113	1	0.4213	1	0.795
	High	256	1.2		1.038	
G3195	Low	206	1	<0.0001	1	0.0001
	High	163	3.238		1.662	
G3560	Low	246	1	<0.0001	1	<0.0001
	High	123	4.209		1.74	
G2114	Low	275	1	0.0056	1	0.1627
	High	94	1.776		1.232	
G1809	Low	238	1	0.0027	1	0.055
	High	131	1.824		1.306	
G3341	Low	188	1	<0.0001	1	0.0005
	High	181	3.185		1.592	
G1590	Low	167	1	0.0956	1	0.9102
	High	202	1.413		0.985	
G1362	Low	261	1	0.0399	1	0.0004
	High	108	1.526		1.634	
G3865	Low	192	1	<0.0001	1	0.0014
	High	177	3.145		1.532	

standard tests (χ^2 , t test) where appropriate using StatView 5.0 for Windows (SAS Institute, Cary, NC). Significance was defined as $P < 0.05$.

Results

Profiling of Human Serum Glycoforms and ROC Analysis in HCC Patients and Normal Controls. N-glycan profiles of blood samples from our HCC cohort were obtained by MALDI-TOF MS analysis using the high-throughput features of the instrument. We thereby identified 67 N-glycans from which we selected molecules that showed statistical differences by ROC analysis between HCC and disease-free individuals (normal controls, NC) comprising living related liver transplantation donors. Glycans with an AUC value greater than 0.80 were selected for analysis (Table 1) and boxplots for these selected molecules (14 in total) are shown in Fig. 1. Clear differences in the distribution of these factors are evident between the NC and HCC patients. The cutoff values were determined using the maximum values for specificity plus sensitivity. G2890 was elevated more than a cutoff value in 305 (82.7%) of HCC patients and G3560 in 261 (70.7%).

Causes of Death. There were 115 deaths in total among our 369 HCC patient cohort (31.2%). The causes of death were as follows: HCC recurrence ($n = 97$; 84.3%), liver failure ($n = 6$; 5.2%), and other causes ($n = 12$; 10.4%).

Univariate Analysis and Multivariate Analysis of Overall Patient and Disease-Free Survival. The overall PS rates at 1, 3, and 5 years in our HCC cohort were 88.8%, 76.4%, and 67.6%, respectively. The DFS values for this groups at 1, 3, and 5 years were 64.0%, 35.5%, and 27.4%, respectively. The 14 serum N-glycans that were highly specific for HCC were evaluated for 3-year recurrence-free survival by ROC analysis to determine the cutoff values about these N-glycans. The patients were divided to two groups by these cutoff values. The PS and DFS measurements associated with the selected 14 selected N-glycans were evaluated by univariate analysis. The P values for the PS rates associated with G2890, G1708, G3195, G3560, G2114, G1809, G3341, G1362, and G3865 were all less than 0.05. The DFS P values for G2890, G1708, G3195, G3560, G3341, G1362, and G3865 were also less than 0.05 (Table 2). When clinical and tumor-associated factors were evaluated by univariate analysis, albumin, Child-Pugh classification,

Table 3. Univariate Analysis of Predictive Values (Clinical and Tumor Associated Factors) for Patient Survival (PS) and Disease-Free Survival (DFS)

		(n)	PS Hazard Ratio	PS P-value	DFS Hazard Ratio	DFS P-value
Sex	Male	301	1	0.7486	1	0.6535
	Female	68	0.913		0.943	
Age (years)	≤62	160	1	0.3272	1	0.6320
	62<	209	1.211		1.106	
HBV	Positive	176	1.259	0.1911	1.007	0.8093
	Negative	192	1		1	
HCV	Positive	119	1.291	0.2433	1.008	0.8183
	Negative	250	1		1	
Albumin (mg/dL)	≤4.05	147	2.128	<0.0001	1.626	0.0001
	4.05<	222	1		1	
Total bilirubin (mg/dL)	≤0.82	235	1	0.5831	1	0.5241
	0.82<	134	1.122		1.128	
ICGR15 (%)	≤16.7	223	1	0.1223	1	0.0106
	16.7<	146	1.349		1.375	
Child-Pugh	A	358	1	<0.0001	1	0.0374
	B	11	4.292		2.169	
Anatomical resection	Anatomical	282	1	0.8569	1	0.1435
	Nonanatomical	87	0.949		1.225	
AFP (ng/mL)	≤20	183	1	<0.0001	1	0.0008
	20<≤1000	115	2.395		1.449	
	1000<	71	4.433		1.870	
AFP-L3 (%)	≤15	255	1	<0.0001	1	0.0567
	15<	113	2.366		1.285	
PIVKA-II (mAU/mL)	≤40	109	1	<0.0001	1	0.0095
	40<≤1000	133	1.593		1.240	
	1000<	123	3.784		1.635	
Number	Single	235	1	<0.0001	1	<0.0001
	2,3	89	3.731		2.252	
	4<=	45	7.299		3.788	
Size (cm)	≤3	116	1	<0.0001	1	0.0086
	3<≤5	96	2.688		1.260	
	5<	157	4.049		1.570	
Differentiation	Well	17	1	0.0003	1	0.0002
	Moderately	190	2.568		2.990	
	Poorly	159	5.358		4.361	
Vp	Positive	94	4.630	<0.0001	2.156	<0.0001
	Negative	275	1		1	
Vv	Positive	35	5	<0.0001	1.969	0.0004
	Negative	334	1		1	
Macroscopic vascular invasion	Positive	48	6.135	<0.0001	1.961	<0.0001
	Negative	321	1		1	
Stage	1	26	1	<0.0001	1	<0.0001
	2	172	2.844		1.206	
	3	111	9.901		2.404	
	4A	60	15.625		3.106	
Noncancerous liver	Cirrhosis	120	1.199	0.3105	1.293	0.0398
	Noncirrhosis	249	1		1	

AFP, alpha-fetoprotein; PIVKA-II, protein induced by vitamin K absence or antagonism factor II; AFP-L3, lens culinaris agglutinin-reactive fraction of alpha-fetoprotein; vp, microscopic tumor thrombus in the portal vein; vv, microscopic tumor thrombus in the hepatic vein; HBV, hepatitis B virus s antigen; HCV, anti-hepatitis C virus antibody; ICGR15, indocyanin green retention rate at 15 minutes.

AFP, AFP-L3 (lens culinaris agglutinin-reactive fraction of alpha-fetoprotein), PIVKA-II, tumor number, tumor size, differentiation, microscopic portal vein invasion, microscopic hepatic vein invasion, macroscopic vascular invasion, and stage were found to be significantly associated with the PS rate. When the same analysis was undertaken for the DFS rate by univariate analysis, albumin, indocyanin green retention rate at

15 minutes, Child-Pugh classification, AFP, PIVKA-II, tumor number, tumor size, differentiation, microscopic portal vein invasion, microscopic hepatic vein invasion, macroscopic vascular invasion, stage, and noncancerous liver were found to be significantly associated with this measure (Table 3).

The variable selection from 19 clinical and tumor-associated factors in Table 3 and the 14 serum

Table 4. Multivariate Analysis of Values That Is Predictive for Overall HCC Patient Survival

		P	Hazard Ratio	95% Confidence Interval	
ICGR15 (%)	16.7<	0.000209	2.435	1.5213	3.898
Child-Pugh	B	0.011136	3.007	1.2852	7.037
AFP (ng/mL)	20<<=1000	0.0003	2.558	1.5372	4.256
	1000<	0.000217	2.782	1.6177	4.786
Tumor number	2,3	0.011844	1.937	1.1575	3.241
	4<=	<0.0001	2.989	1.7693	5.049
Size (cm)	3<<=5	0.278625	1.483	0.7269	3.026
	5<	0.016071	2.237	1.1613	4.307
Vp	Positive	<0.0001	2.982	1.8446	4.822
C3560	>0.158	<0.0001	2.52	1.6191	3.923

ICGR15, indocyanin green retention rate at 15 minutes, AFP, alpha-fetoprotein; vp, microscopic tumor thrombus in the portal vein.

Table 5. Multivariate Analysis of Values That Are Predictive of Disease-Free Survival in HCC Patients

		P	Hazard Ratio	95% Confidence Interval	
ICGR15 (%)	16.7<	0.00334	1.519	1.149	2.008
AFP (ng/mL)	20<<=1000	0.04904	1.366	1.001	1.864
	1000<	0.01851	1.591	1.081	2.342
Tumor number	2,3	0.0072	1.551	1.126	2.135
	4<=	<0.0001	2.649	1.704	4.118
Differentiation	Moderately	0.01495	2.838	1.225	6.577
	Poor	0.00501	3.398	1.446	7.984
vp	Positive	0.01023	1.544	1.108	2.152
C2890	>1.12	0.01125	1.443	1.087	1.915

ICGR15, indocyanin green retention rate at 15 minutes, AFP, alpha-fetoprotein; vp, microscopic tumor thrombus in the portal vein.

N-glycans using the AIC was performed and the selected variables were analyzed with PS and DFS by multivariate analysis. G3560 were found to be independent risk factors for PS (Table 4) and G2890 for DFS (Table 5).

The PS rates of HCC cases with low serum G3560 levels at 5 years were 80.5% and of high serum G3560 at 5 years were 40.4%. The DFS outcomes associated with low and high serum G2890 levels at 5 years were 21.3% and 35.1%, respectively (Fig. 2).

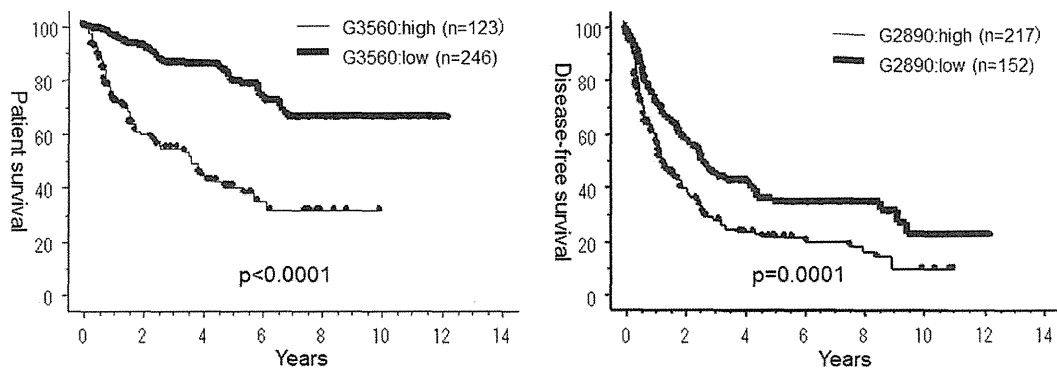


Fig. 2. The PS rates of HCC cases with low and high serum G3560 levels at 5 years were 80.5% and 40.4%, respectively. The DFS outcomes associated with low and high serum G2890 levels at 5 years were 21.3% and 35.1%, respectively.

Relationship Between Clinical and Tumor-Associated Factors in HCC and Specific Glycans.

Among the low and high G2890 HCC groups, there were significant differences found in a number of clinical and tumor-associated factors including albumin, Child-Pugh classification, AFP, PIVKA-II, tumor number, tumor size, microscopic portal vein invasion, microscopic hepatic vein invasion, macroscopic vascular invasion, and stage (Table 6). In comparing the low and high G3560 HCC patients, significant differences were found in albumin, Child-Pugh Classification, operative procedures, AFP, AFP-L3, PIVKA-II, tumor number, tumor size, differentiation profiles, microscopic portal vein invasion, microscopic hepatic vein invasion, macroscopic vascular invasion, and stage (Table 6).

Discussion

The N-glycan profiles of a large cohort of HCC patients were obtained in our current study by MALDI-TOF MS analysis and 67 of these molecules were thereby quantified. Of this group of factors, 14 N-glycans showed higher relative peaks in the HCC patients compared with normal controls and were

Table 6. Correlation Between the G2890 and G3560 *N*-Glycans and Clinical and Tumor Associated Factors in HCC Cases

		G2890		P	G3560		P
		High (n=217)	Low (n=152)		High (n=123)	Low (n=246)	
Sex	Male	184	117	0.0767	105	196	0.2286
	Female	33	35		18	50	
Age	≤62	90	70	0.4433	49	111	0.393
	>62	127	82		74	135	
HBV	Positive	107	69	0.5254	59	117	0.9706
	Negative	110	83		64	129	
HCV	Positive	63	56	0.1425	32	87	0.0904
	Negative	154	96		91	159	
Albumin (mg/dL)	≤4.05	109	38	<0.0001	73	74	<0.0001
	>4.05	108	114		50	172	
Total bilirubin (mg/dL)	≤0.82	136	99	0.7088	82	153	0.4671
	>0.82	81	53		41	93	
ICGR15 (%)	≤16.7	125	98	0.2224	77	146	0.6246
	>16.7	92	54		46	100	
Child-Pugh	A	206	152	0.0034	115	243	0.008
	B	11	0		8	3	
Anatomical resection	Anatomical	172	110	0.1583	106	176	0.0028
	Nonanatomical	45	42		17	70	
AFP (ng/mL)	≤20	102	81	0.0461	52	131	<0.0001
	20< & ≤1000	64	51		30	85	
	>1000	51	20		41	30	
AFP-L3 (%)	≤15	143	112	0.1147	68	187	<0.0001
	>15	74	40		55	59	
PIVKA II (mAU/mL)	≤40	52	58	0.0001	22	88	<0.0001
	40< & ≤1000	74	60		33	101	
	>1000	91	34		68	57	
Number	Single	122	113	0.0009	68	167	<0.0001
	2, 3	60	29		27	62	
Size (cm)	≤4	35	10	<0.0001	28	17	<0.0001
	≤3	48	68		15	101	
	3< & ≤5	60	36		21	75	
Differentiation	>5	109	48	0.0981	87	70	0.0003
	Well	12	8		6	14	
vp	Moderately	102	88	0.0065	46	144	<0.0001
	Poorly	103	56		71	88	
	Positive	67	27		49	45	
w	Negative	150	125	0.0043	74	201	<0.0001
	Positive	29	6		24	11	
Macroscopic vascular invasion	Negative	188	146	<0.0001	99	235	<0.0001
	Positive	43	5		32	16	
Stage	Negative	174	147	<0.0001	91	230	<0.0001
	1	7	19		3	23	
	2	88	84		45	127	
	3	71	40		35	76	
	4A	51	9		40	20	
Noncancerous liver	Cirrhosis	71	49	0.9876	35	85	0.2888
	Noncirrhosis	146	103		88	161	

AFP, alpha-fetoprotein; PIVKA-II, protein induced by vitamin K absence or antagonism factor II; AFP-L3, lens culinaris agglutinin-reactive fraction of alpha-fetoprotein; vp, microscopic tumor thrombus in the portal vein; w, microscopic tumor thrombus in the hepatic vein; HBV, hepatitis B virus s antigen; HCV, anti-hepatitis C virus antibody; ICGR15, indocyanin green retention rate at 15 minutes.

chosen for further analysis. These selected molecules were assessed for any correlation with surgical outcomes in the HCC cohort (i.e., prognosis and recurrence) by univariate and multivariate analysis. G3560 *N*-glycan was found to be a significant prognostic factor and G2890 *N*-glycan was found to be a significant recurrence factor for this disease. Moreover, G2890 and G3560 were found to strongly correlate with a

number of well-known tumor-related prognostic and recurrent factors. These results show that quantitative glyco blotting based on whole serum *N*-glycan profiling is a potent screening approach for novel HCC biomarkers, and that the G3560 and G2890 *N*-glycans are promising biomarkers of the PS, DFS, and malignant behavior characteristics of HCC after hepatectomy.

Although glycans, once released from glycoproteins or glycopeptides, have been subjected to fluorescent labeling and purification for detection by high-performance liquid chromatography (HPLC) previously, this method is time-consuming and therefore not suited to clinical diagnosis. Our novel analytical method, which we refer to as glycoblotting, is far more rapid and accurate, as evidenced by the number of *N*-glycans detected in our current analysis. This chemoselective glycan enrichment technology known as glycoblotting was developed in our laboratory to purify oligosaccharides derived from glycoproteins in an effective and quantitative manner, thus enabling serum glycan profiling by way of a simpler method.²⁰ Our method is also applicable to the fully automated analysis of multiple samples simultaneously. It readily combines the isolation and labeling of oligosaccharides, which can then be subjected to conventional analytical methods including MS. We had already achieved high-speed quantitative and qualitative profiling of glycan expression patterns in biological materials using this technology. In our present study, we improved the method to allow quantitative analysis of high reproducibility and accuracy using a calibration curve of human serum standards. The analysis of the obtained 67 glycan profiles was performed using this new developed technology. The effectiveness of our method is evidenced by the identification of the G2890 and G3560 *N*-glycans as highly promising clinical markers of HCC associated with the PS, DFS, and tumor malignancy rates of these cancers.

It has been reported that AFP is the most significant tumor marker and independent predictor of prognosis for HCC,²⁶ even in patients who have received a hepatectomy.²⁷ Although high levels of AFP in cases of fully developed HCC, or in the serum of the host, are known to be associated with more aggressive behavior, and increased anaplasia,²⁸ AFP can also cause apoptosis in tumor cells.²⁹ Moreover, it has been suggested that AFP regulates the immune response and induces either stimulatory or inhibitory growth activity.³⁰ On the other hand, it is well known that AFP may increase in some patients with acute and chronic hepatitis without HCC,^{31,32} and that the elevation of AFP correlates with inflammation of background disease and hepatocyte regeneration.³³ Hence, because the AFP profile does not always directly reflect the extent of tumor malignancy, the AFP levels do not influence patient survival and recurrence. On the other hand, AFP and many important tumor markers, such as carcinoembryonic antigen, carbohydrate antigen 125, and carbohydrate antigen 19-9, are glycoproteins, and this

means that the glycan profiles in serum are altered by the onset of cancer. Indeed, the profiling of serum glycans has been performed previously as a screen for distinct potential glycan biomarkers of ovarian cancer and breast cancer.^{18,19} Hence, we surmised that highly specific glycoprotein markers of HCC should be detected by monitoring the serum glycosylation profile in these patients. In glycan structure, both G2890 and G3560 are multiply branched (G2890 is tri-antennary and G3560 is tetra-antennary) glycans with a core fucose. In addition, both glycans have one nonsialylated branch, i.e., G2890 and G3560, are tri-antennary disialylated glycan, and tetra-antennary tri-sialylated glycan, respectively. The structure of G2890 and G3560 is quite different from the AFC-L3 (core fucosylated bi-antennary glycan) and CA19-9 (sialylated Lewis (a) antigen), which are well-known biomarkers related to HCC except for the core fucosylation.

There have been several previous studies of glycans in HCC. Kudo et al.³⁴ reported that *N*-glycan alterations are associated with drug resistance in HCC *in vitro*. In other reported clinical studies, only specific glycans have been assessed in relation to HCC. Vanhooren et al.¹⁷ were the first to analyze the function of HCC-specific glycans, and reported that a triantennary glycan (NA-3Fb) correlated with the tumor stage and AFP levels in HCC patients. However, that study analyzed 44 patients with HCC but did not evaluate the relationship between the *N*-glycans and the clinical and pathological factors of this disease, the clinical course after hepatectomy, or prognosis and recurrence. In our current study, in contrast, we analyzed a far larger cohort than any other previous report, and evaluated a comprehensive panel of clinical and pathological parameters in relation to the *N*-glycan profile in HCC. Tang et al.³⁵ also described some HCC-specific glycans in their previous study that we did not find to be significant in our current analyses. This is likely due to the fact that the patient number in their study was smaller than ours, and the fact that the *N*-glycome profile in serum is gender- and age-dependent.³⁶ In this study, the mean age and the distribution of gender and infection of hepatitis B and C virus were the difference between NC and HCC patients. However, the selected 14 serum *N*-glycans were quantified by our MALDI-TOF MS analysis and compared with NC by ROC analysis. These were statistically different between HCC and NC with respect to the quantity. Because these 14 serum *N*-glycans of which the AUC values were greater than 0.80 were revealed to be specific for HCC, they had a high discriminating ability to differentiate HCC from NC. Further analyses are

required to determine whether G2890 and G3560 are elevated in patients with hepatitis B, hepatitis C, and/or cirrhosis without HCC.

The most important adverse prognostic factor for liver resection and transplantation in HCC has been found to be microscopic venous invasion.⁵ However, microscopic portal invasion is not diagnosed preoperatively, and is revealed only by pathological examination. New biomarkers that are more strongly associated with prognosis and recurrence of HCC than AFP, AFP-L3, or PIVKA-II are therefore highly desirable. Our current data show that the *N*-glycans G2890 and G3560 correlate closely with well-known tumor-related prognostic and recurrent factors such as tumor number, size, microscopic portal vein invasion, microscopic hepatic vein invasion, differentiation, macroscopic vascular invasion, stage, AFP, AFP-L3, and PIVKA-II (Table 6). Moreover, when G2890 and G3560 were simultaneously included in multivariate analysis for PS and DFS with AFP, AFP-L3 and PIVKA-II, *P*-values of G2890 and G3560 were lower than AFP, and AFP-L3, and PIVKA-II were not selected as valuables by AIC. We demonstrate that these are novel independent prognostic factors for HCC that are related to the survival and recurrence of this disease and that show a lower *P*-value than other established tumor factors. Hence, we predict that G2890 and G3560 will prove to be markers that can preoperatively predict HCC tumor malignancy including microscopic portal vein invasion, and the PS and DFS rates more accurately and with more potency than the more well-known biomarkers.

Acknowledgment: We thank the staff of the Gastroenterological Surgery I, Graduate School of Medicine, and Faculty of Advanced Life Science, Frontier Research Center for Post-Genome Science and Technology, Hokkaido University, and System Instruments Co. Ltd., Science & Technology Systems Inc., Bruker Daltonics K. K., for their kind cooperation during this study.

References

- Farazi PA, DePinho RA. Hepatocellular carcinoma pathogenesis: from genes to environment. *Nat Rev Cancer* 2006;6:674-687.
- Arii S, Yamaoka Y, Futagawa S, Inoue K, Kobayashi K, Kojiro M, et al. Results of surgical and nonsurgical treatment for small-sized hepatocellular carcinomas: a retrospective and nationwide survey in Japan. The Liver Cancer Study Group of Japan. *HEPATOLOGY* 2000;32:1224-1229.
- Hasegawa K, Kokudo N, Imamura H, Matsuyama Y, Aoki T, Minagawa M, et al. Prognostic impact of anatomic resection for hepatocellular carcinoma. *Ann Surg* 2005;242:252-259.
- Kamiyama T, Nakanishi K, Yokoo H, Kamachi H, Tahara M, Suzuki T, et al. Recurrence patterns after hepatectomy of hepatocellular carcinoma: implication of Milan criteria utilization. *Ann Surg Oncol* 2009;16:1560-1571.
- Ikai I, Arii S, Kojiro M, Ichida T, Makuuchi M, Matsuyama Y, et al. Reevaluation of prognostic factors for survival after liver resection in patients with hepatocellular carcinoma in a Japanese nationwide survey. *Cancer* 2004;101:796-802.
- Shah SA, Cleary SP, Wei AC, Yang I, Taylor BR, Hemming AW, et al. Recurrence after liver resection for hepatocellular carcinoma: risk factors, treatment, and outcomes. *Surgery* 2007;141:330-339.
- Imamura H, Matsuyama Y, Miyagawa Y, Ishida K, Shimada R, Miyagawa S, et al. Prognostic significance of anatomical resection and des-gamma-carboxy prothrombin in patients with hepatocellular carcinoma. *Br J Surg* 1999;86:1032-1038.
- Shimada M, Takenaka K, Fujiwara Y, Gion T, Kajiyama K, Maeda T, et al. Des-gamma-carboxy prothrombin and alpha-fetoprotein positive status as a new prognostic indicator after hepatic resection for hepatocellular carcinoma. *Cancer* 1996;78:2094-2100.
- Shirabe K, Itoh S, Yoshizumi T, Soejima Y, Taketomi A, Aishima S, et al. The predictors of microvascular invasion in candidates for liver transplantation with hepatocellular carcinoma—with special reference to the serum levels of des-gamma-carboxy prothrombin. *J Surg Oncol* 2007;95:235-240.
- Esnaola NF, Lauwers GY, Mirza NQ, Nagorney DM, Doherty D, Ikai I, et al. Predictors of microvascular invasion in patients with hepatocellular carcinoma who are candidates for orthotopic liver transplantation. *J Gastrointest Surg* 2002;6:224-232; discussion 232.
- Tamura S, Kato T, Berho M, Misiakos EP, O'Brien C, Reddy KR, et al. Impact of histological grade of hepatocellular carcinoma on the outcome of liver transplantation. *Arch Surg* 2001;136:25-30; discussion 31.
- Toyoda H, Kumada T, Kiriya S, Sone Y, Tanikawa M, Hisanaga Y, et al. Prognostic significance of simultaneous measurement of three tumor markers in patients with hepatocellular carcinoma. *Clin Gastroenterol Hepatol* 2006;4:111-117.
- Inoue S, Nakao A, Harada A, Nonami T, Takagi H. Clinical significance of abnormal prothrombin (DCP) in relation to postoperative survival and prognosis in patients with hepatocellular carcinoma. *Am J Gastroenterol* 1994;89:2222-2226.
- Imamura H, Matsuyama Y, Tanaka E, Ohkubo T, Hasegawa K, Miyagawa S, et al. Risk factors contributing to early and late phase intrahepatic recurrence of hepatocellular carcinoma after hepatectomy. *J Hepatol* 2003;38:200-207.
- Sumie S, Kuromatsu R, Okuda K, Ando E, Takata A, Fukushima N, et al. Microvascular invasion in patients with hepatocellular carcinoma and its predictable clinicopathological factors. *Ann Surg Oncol* 2008;15:1375-1382.
- Kang P, Madera M Jr WRA, Goldman R, Mechref Y, Novotny MV. Glycomic alterations in the highly-abundant and lesser-abundant blood serum protein fractions for patients diagnosed with hepatocellular carcinoma. *Int J Mass Spectrom* 2011;305:185-198.
- Vanhooren V, Liu XE, Franceschi C, Gao CF, Libert C, Contreras R, et al. N-glycan profiles as tools in diagnosis of hepatocellular carcinoma and prediction of healthy human ageing. *Mech Ageing Dev* 2009;130:92-97.
- Kirmiz C, Li B, An HJ, Clowers BH, Chew HK, Lam KS, et al. A serum glycomics approach to breast cancer biomarkers. *Mol Cell Proteomics* 2007;6:43-55.
- An HJ, Miyamoto S, Lancaster KS, Kirmiz C, Li B, Lam KS, et al. Profiling of glycans in serum for the discovery of potential biomarkers for ovarian cancer. *J Proteome Res* 2006;5:1626-1635.
- Miura Y, Hato M, Shinohara Y, Kuramoto H, Furukawa J, Kuroguchi M, et al. BlotGlycoABCTM, an integrated glycoblotting technique for rapid and large scale clinical glycomics. *Mol Cell Proteomics* 2008;7:370-377.
- Nishimura S, Niikura K, Kuroguchi M, Matsushita T, Fumoto M, Hinou H, et al. High-throughput protein glycomics: combined use of

- chemoselective glycoblotting and MALDI-TOF/TOF mass spectrometry. *Angew Chem Int Ed Engl* 2004;44:91-96.
22. Furukawa J, Shinohara Y, Kuramoto H, Miura Y, Shimaoka H, Kuroguchi M, et al. Comprehensive approach to structural and functional glycomics based on chemoselective glycoblotting and sequential tag conversion. *Anal Chem* 2008;80:1094-1101.
 23. Ichida F, Tsuji T, Omata M, Ichida T, Inoue K, Kamimura T, et al. New Inuyama Classification; new criteria for histological assessment of chronic hepatitis. *Int Hepatol Commun* 1996;6:112-119.
 24. The Liver Study Group of Japan. The general rules for the clinical and pathological study of primary liver cancer. 3rd English ed. Tokyo, Japan: Kanehara & Co.
 25. Akaike H. A new look at the statistical model identification. *IEEE Trans Autom Control* 1974;19:716-723.
 26. Nomura F, Ohnishi K, Tanabe Y. Clinical features and prognosis of hepatocellular carcinoma with reference to serum alpha-fetoprotein levels. Analysis of 606 patients. *Cancer* 1989;64:1700-1707.
 27. Hanazaki K, Kajikawa S, Koide N, Adachi W, Amano J. Prognostic factors after hepatic resection for hepatocellular carcinoma with hepatitis C viral infection: univariate and multivariate analysis. *Am J Gastroenterol* 2001;96:1243-1250.
 28. Matsumoto Y, Suzuki T, Asada I, Ozawa K, Tobe T, Honjo I. Clinical classification of hepatoma in Japan according to serial changes in serum alpha-fetoprotein levels. *Cancer* 1982;49:354-360.
 29. Yang X, Zhang Y, Zhang L, Mao J. Silencing alpha-fetoprotein expression induces growth arrest and apoptosis in human hepatocellular cancer cell. *Cancer Lett* 2008;271:281-293.
 30. Mizejewski GJ. Alpha-fetoprotein structure and function: relevance to isoforms, epitopes, and conformational variants. *Exp Biol Med (Maywood)* 2001;226:377-408.
 31. Smith JB. Occurrence of alpha-fetoprotein in acute viral hepatitis. *Int J Cancer* 1971;8:421-424.
 32. Silver HK, Gold B, Shuster J, Javitt NB, Freedman SO, Finlayson ND. Alpha(1)-fetoprotein in chronic liver disease. *N Engl J Med* 1974;291:506-508.
 33. Fujiyama S, Tanaka M, Maeda S, Ashihara H, Hirata R, Tomita K. Tumor markers in early diagnosis, follow-up and management of patients with hepatocellular carcinoma. *Oncology* 2002;62(Suppl 1):57-63.
 34. Kudo T, Nakagawa H, Takahashi M, Hamaguchi J, Kamiyama N, Yokoo H, et al. N-glycan alterations are associated with drug resistance in human hepatocellular carcinoma. *Mol Cancer* 2007;6:32.
 35. Tang Z, Varghese RS, Bekesova S, Loffredo CA, Hamid MA, Kyselova Z, et al. Identification of N-glycan serum markers associated with hepatocellular carcinoma from mass spectrometry data. *J Proteome Res* 2010;9:104-112.
 36. Ding N, Nie H, Sun X, Sun W, Qu Y, Liu X, et al. Human serum N-glycan profiles are age and sex dependent. *Age Ageing* 2011;40:568-575.

High Expression of MicroRNA-210 is an Independent Factor Indicating a Poor Prognosis in Japanese Triple-negative Breast Cancer Patients

Tatsuya Toyama^{1,*}, Naoto Kondo¹, Yumi Endo¹, Hiroshi Sugiura¹, Nobuyasu Yoshimoto¹, Mai Iwasa¹, Satoru Takahashi^{2,3}, Yoshitaka Fujii¹ and Hiroko Yamashita¹

¹Department of Oncology, Immunology and Surgery, Nagoya City University Graduate School of Medical Sciences, 1 Kawasumi, Mizuho-cho, Mizuho-ku, ²Department of Experimental Pathology and Tumor Biology, Nagoya City University Graduate School of Medical Sciences, 1 Kawasumi, Mizuho-cho, Mizuho-ku and ³Division of Pathology, Nagoya City University Hospital, 1 Kawasumi, Mizuho-cho, Mizuho-ku, Nagoya 467-8601, Japan

*For reprints and all correspondence: Tatsuya Toyama, Department of Oncology, Immunology and Surgery, Nagoya City University Graduate School of Medical Sciences, 1 Kawasumi, Mizuho-cho, Mizuho-ku, Nagoya 467-8601, Japan. E-mail: toyamat-ncu@umin.ac.jp

Received September 29, 2011; accepted January 3, 2012

Objective: MicroRNAs have emerged as a new class of non-coding genes involved in regulating cell proliferation, differentiation and viability. Recent studies have identified miR-210 as one of a set of hypoxia-regulated microRNAs and demonstrated a direct regulatory role of HIF-1 alpha for its transcription. Here, we assessed miR-210 expression in Japanese triple-negative breast cancers and determined its clinical significance.

Methods: TaqMan MicroRNA assays for miR-210 expression were performed on 161 samples of Japanese breast cancer tissue (58 triple-negative breast cancer and 103 estrogen receptor positive/HER2 negative). Correlations between miR-210 expression and clinicopathological factors were analyzed. The effects of several variables on survival were tested by a Cox proportional hazards regression analysis.

Results: miR-210 expression in triple-negative breast cancers was significantly higher than in estrogen receptor-positive/HER2-negative breast cancers ($P < 0.001$). Patients whose triple-negative breast cancers showed low miR-210 expression experienced significantly better disease-free and overall survival than those with high miR-210 expression ($P = 0.02$ and $P = 0.05$, respectively). Although the prognosis of patients with triple-negative breast cancers is poor, Cox univariate and multivariate analyses demonstrated that a higher expression of miR-210 was an independent factor indicating a worse prognosis than for patients with a low level of miR-210.

Conclusions: The degree of miR-210 expression might be a clinically useful prognostic factor for decision-making regarding treatment in the adjuvant setting, especially in node-negative triple-negative breast cancer patients.

Key words: microRNA – miR-210 – breast cancer – triple negative